

## **Bridging the Gap:**

# Connecting Atomic Nuclei to Their Quantum Foundations

#### Fredrick Olness\*

Department of Physics, Southern Methodist University, Dallas, TX 75275-0175, U.S.A.

E-mail: olness@smu.edu

We extend the QCD Parton Model analysis by employing a factorized nuclear structure model that explicitly accounts for both individual nucleons and correlated nucleon pairs. This novel framework establishes a paradigm that directly links the nuclear physics description of matter (in terms of protons and neutrons) to the particle physics schema (in terms of quarks and gluons). Our analysis of high-energy data from lepton Deep-Inelastic Scattering, Drell-Yan, and W/Z production simultaneously extracts the universal effective distribution of quarks and gluons inside correlated nucleon pairs, and their nucleus-specific fractions. The successful extraction of these universal distributions marks a significant advance in our understanding of nuclear structure, as it directly connects nucleon-level and parton-level quantities.

XXXII International Workshop on Deep Inelastic Scattering and Related Subjects (DIS2025) 24-28 March, 2025 Cape Town, South Africa

<sup>&</sup>lt;sup>†</sup>Performed in collaboration with A.W. Denniston, T. Ježo, A. Kusina, N. Derakhshanian, P. Duwentäster, O. Hen, C. Keppel, M. Klasen, K. Kovařík, J.G. Morfín, K.F. Muzakka, E. Piasetzky, P. Risse, R. Ruiz, I. Schienbein, J.Y. Yu. 
\*Speaker

#### A Novel Paradigm:

Subatomic systems—including nucleons and atomic nuclei, as well as dense astrophysical matter—derive their fundamental properties from the complex, many-body interactions among their constituent quarks and gluons, all of which are precisely described by the theory of Quantum Chromodynamics (QCD).

We present a novel framework that combines information from nuclear Parton Distribution Functions (nPDFs) with Short-Range Correlations (SRCs)<sup>1</sup>. This approach directly establishes a crucial link between partonic dynamics (quarks and gluons) and nuclear dynamics (protons and neutrons).

The PDFs are a key component that allows us to describe the complex internal structure and interactions of nuclei. Notably, the nuclear PDFs are not a simple sum of the PDFs for free protons and neutrons [2, 3]. Instead, they demonstrate significant nuclear modification effects (such as the EMC effect, shadowing, and antishadowing) that alter the momentum distributions of quarks and gluons inside a nucleus relative to those in individual nucleons.

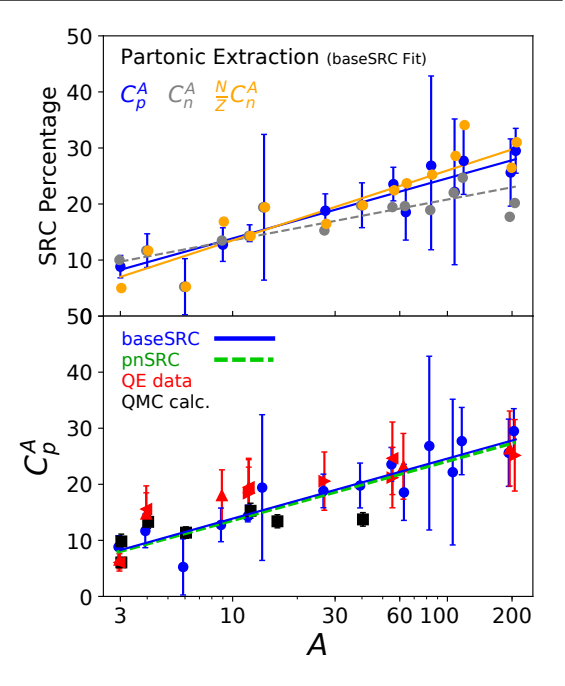


**Figure 1:** (a) Comparison of nuclear structure parameters  $C_p^A$ ,  $C_n^A$ , and  $(N/Z)C_n^A$  values for the baseSRC fit. The solid lines represent logarithmic fits to the corresponding quantities. We show uncertainties only for the  $C_p^A$ , but errors for other quantities are of similar size.

(b) Comparison of  $C_p^A$  values for the baseSRC fit and the SRC abundances extracted from quasi-elastic (QE) [4–6] data and Quantum Monte Carlo (QMC) [7] nuclear calculations. The logarithmic fits for baseSRC and pnSRC are also shown.

#### nPDF Framework:

We adopt a model-agnostic approach by focusing on the broad-scale features common to modern, high-resolution nuclear structure models, thereby minimizing dependence on specific model details. The parameterization framework for the nuclear Parton Distribution Functions (nPDFs) differs significantly from those employed in conventional global analyses. Nevertheless, it achieves a notably good description of the currently available nuclear data, as we shall demonstrate.

We construct our nPDF as a linear combination of a free-nucleon PDF (which accounts for the quasi-free nucleons) and a universal Short-Range Correlation (SRC) PDF that describes the quark and gluon distributions inside an SRC pair:

$$f_i^A(x,Q) = \frac{Z}{A} \left[ (1 - C_p^A) f_i^p(x,Q) + C_p^A f_i^{SRC \, p}(x,Q) \right] + \frac{N}{A} \left[ (1 - C_n^A) f_i^n(x,Q) + C_n^A f_i^{SRC \, n}(x,Q) \right].$$

Here,  $f_i^A$  is the nPDF of parton type i (gluon or quark flavors) in a nucleus with mass number A, carrying momentum fraction x at energy scale Q.  $f_i^{P,n}$  and  $f_i^{SRC\,P,n}$  are the PDFs of the free-nucleon and of the modified nucleon in an SRC pair, respectively. We implicitly assume that

<sup>&</sup>lt;sup>1</sup>For a complete list of references, please refer to those cited in Ref. [1]

 $f_i^{SRC\,p,n}$  can be defined via a collinear factorization framework, and that the proton and neutron distributions are related by isospin.<sup>2</sup> Therefore, we apply the tools from perturbative QCD used for free-nucleon PDFs to arrive at the physical predictions.

A crucial characteristic of SRCs is their universality across the full nuclear spectrum, meaning the short-distance dynamics of the correlated pairs are largely independent of the specific nucleus.

We keep a model-independent approach as to the number of SRC pairs and their isospin structure. The nuclear structure dependence is fully encapsulated in the fraction of nucleons in SRC pairs, denoted by  $C_{p,n}^A$  [1, 8]. In fact, these nuclear structure parameters  $C_{p,n}^A$  will be independently determined in our nPDF analysis for the first time (cf., Fig. 1), and tested for consistency with independent results from specific nuclear structure studies.

#### **nPDF** Analysis::

The analysis utilized the full set of available data on nuclear lepton DIS, Drell-Yan processes, and W and Z boson production. The corresponding theoretical predictions were obtained at next-to-leading order (NLO) in QCD. The DIS data primarily constrain the u and d quark and anti-quark distributions. In contrast, the W and Z boson production data from LHC proton-

$\chi^2/N_{\rm data}$	DIS	DY	W/Z	JLab	$\chi^2_{ m tot}$	$\frac{\chi^2_{ m tot}}{N_{ m DOF}}$
traditional	0.85	0.97	0.88	0.72	1408	0.85
baseSRC	0.84	0.75	1.11	0.41	1300	0.80
pnSRC	0.85	0.84	1.14	0.49	1350	0.82
$N_{ m data}$	1136	92	120	336	1684	

**Table 1:** The partial  $\chi^2/N_{\rm data}$  values for the data subsets; the number of data points ( $N_{\rm data}$ ) for each process are listed in the bottom row. The traditional fit has 19 shape and 3 W/Z normalization parameters. The baseSRC and pnSRC fits have 21 shape, 3 W/Z normalization, and 30 and 19 SRC parameters ( $C_{p,n}^A$ ), respectively. In total, there are 1684 data points after cuts. Note the last column ( $\chi^2_{\rm tot}/N_{\rm DOF}$ ) fully takes into account the number of fit parameters.

lead collisions also constrain strange quark and gluon distributions down to lower momentum fractions of  $x \sim 10^{-3}$ .

The energy-scale dependence is accounted for using the DGLAP evolution equation, which also helps constrain the gluon distribution via the Q-dependence of DIS data. The parton number and momentum sum rules are guaranteed to be satisfied separately for the free-nucleon PDFs  $(f_i^P)$  and for the SRC PDFs  $(f_i^{SRC\,P})$ . Because each component already satisfies these fundamental rules, their linear combination (which forms the total nuclear PDF) must also satisfy the sum rules. This holds independently of the specific values used for the proton and neutron SRC fractions  $(C_p^A)$  and  $C_n^A$ .

The free-nucleon PDFs  $f_i^P$  are set to the nCTEQ15 proton distributions [2]. We have also explored other proton sets from different groups and obtained comparable results. The SRC nucleon PDFs  $f_i^{SRC\ p}$  use the same functional form as  $f_i^P$  with 21 shape parameters. We perform two independent analyses where i)  $C_p^A$  and  $C_n^A$  are allowed to vary freely, and ii) where we assume proton-neutron SRC dominance, i.e.  $C_p^A = \frac{N}{Z} \times C_n^A \equiv C^A$ . We refer to these fits as the baseSRC and pnSRC fits, respectively. For comparison, we also repeated the traditional (mean-field-like) analysis of Ref. [9] using the same dataset, which we refer to as the traditional fit.

<sup>&</sup>lt;sup>2</sup>We will assume isospin symmetry to relate the proton and neutron nPDFs. Therefore, in the following discussion, we will simply use  $f_i^p$  and  $f_i^{SRC p}$  to identify the free-nucleon and SRC nPDFs, respectively.

#### **Analysis Results:**

The  $\chi^2$  Results: The resulting fit quality in terms of  $\chi^2$  are listed in Table 1 for each data type separately, and for all data combined. The SRC fits result in overall  $\chi^2_{\rm tot}/N_{\rm DOF}$  values appreciably better than for the traditional fit; this fully takes into account the additional SRC  $(C_{p,n}^A)$  parameters.

**nPDF Results:** The nPDFs obtained from the SRC approach (not shown) are generally consistent with those from the traditional fits within the estimated uncertainties. The SRC approach not only yields nPDFs that closely reproduce the traditional results (including the most well-constrained valence distributions) but also achieves an improved  $\chi^2$ /dof. This fit successfully reproduces all data across the full range, corresponding to an x range of approximately  $10^{-3}$  to 0.75.

Given that the initial nPDF parameterization in the SRC framework differs fundamentally from the traditional functional form, achieving results comparable to those of the latter while improving data description is a noteworthy achievement.

### The $C_{n,n}^A$ Coefficients:

Figure 1 shows the extracted  $C_p^A$  and  $C_n^A$  coefficients as determined by the global baseSRC. The coefficients show logarithmic growth with the nuclear mass number A, starting from  $\sim 5\%$  for He and reaching  $\sim 25\%$  for Pb.

**Figure 1-a):** In the top panel of Fig. 1-a) we display  $\{C_n^A, C_p^A\}$  for the baseSRC fit. We also show a rescaled coefficient,  $(N/Z)C_n^A$ , that accounts for the neutron excess when present. The uncertainties of  $\{C_n^A, C_p^A\}$  are obtained by evaluating the  $\chi^2$  while scanning across the parameters, and reflect, in part, the number of data points available for each separate nucleus. The lines are simple logarithmic fits to show the trend in A.

We first observe that the slopes of the proton fraction  $(C_p^A)$  and the neutron fraction  $(C_n^A)$  of nucleons in SRC pairs are roughly similar when compared against the nuclear mass number A. However, after accounting for the neutron excess (by multiplying  $C_n^A$  by the factor N/Z), we find that the slopes of  $C_p^A$  and the rescaled  $(N/Z)C_n^A$  become essentially the same within the estimated uncertainties. This result indicates that protons and neutrons participate in the SRC interactions in approximately equal numbers, consistent with the hypothesis that SRCs are dominated by proton–neutron pairs.

Furthermore, the observation that  $C_p^A$  and the rescaled  $(N/Z)C_n^A$  exhibit similar behavior explains why imposing the constraint  $C_p^A = (N/Z)C_n^A$  in the pnSRC fit results in only a minimal increase in  $\chi^2/\text{dof}$  (from 0.80 to 0.82) relative to the baseSRC fit, where  $C_p^A$  and  $C_n^A$  are treated independently.

We note that  $\{C_n^A, C_p^A\}$  exhibit a scaling freedom on their absolute value due to a freedom in the parameterization [8]. Although no evidence of this scaling freedom was identified in our results, we focus the following discussion on the relative size of the coefficients instead of their absolute values.

**Example Nuclei:** For the baseSRC fit, the  $\{C_p^A, C_n^A\}$  vary independently without constraints; hence, the observed trends are purely due to the data. We previously noted that when the obtained

 $\{C_p^A, C_n^A\}$  values are adjusted for the neutron excess present in heavy nuclei, the resulting effective number of protons and neutrons in SRC pairs is approximately equal. We will now illustrate this specific finding for the cases of gold and lead nuclei.

The estimated uncertainties for  $\{C_p^A, C_n^A\}$  are displayed in Fig. 1 for the case of gold and lead are roughly  $\pm 5\%$ . For gold,  $^{197}_{79}$ Au, we obtain  $C_p^A=0.256$ ,  $C_n^A=0.177$ . This implies  $79\times C_p^A\simeq 20.2$  protons and  $118\times C_n^A\simeq 20.9$  neutrons are (effectively) modified by the SRC. Likewise for the case of lead,  $^{208}_{82}$ Pb, we have  $C_p^A=0.295$ ,  $C_n^A=0.202$ , which implies  $82\times C_p^A\simeq 24.2$  protons and  $126\times C_n^A\simeq 25.5$  neutrons are (effectively) modified. This exemplifies the above observation that once the  $C^A$ -coefficients are adjusted to account for the neutron excess, the effective number of protons and neutrons within SRC pairs are approximately equal.

**Proton-Neutron SRC Dominance:** More generally, we find the above pattern or proton-neutron pairing is evident throughout the range of Fig. 1; we fit the  $\{C_p^A, C_n^A\}$  values with a simple 2-parameter function,  $f(A) = a \log(A) + b$ , to better display the trends. In the top panel of Fig. 1 we observe  $C_p^A$  (blue line) and  $C_n^A$  (gray line) are both increasing with A, but with differing slopes.

To account for the abundance of neutrons for non-isoscalar nuclei, we modify the original  $C_n^A$  values by a factor of N/Z, and this yields the orange line with a slope much closer to the  $C_p^A$  slope (blue line). By comparing the rescaled neutron fraction line,  $(N/Z)C_n^A$ , with the original proton fraction line,  $C_p^A$ , we gain insight into two key aspects of the SRCs.

- Proton-Neutron SRC Dominance: The overlap directly shows the extent to which the effective number of protons and neutrons participating in SRC interactions are comparable, after accounting for the nuclear neutron excess.
- 2. Nuclear A-Dependence: The similarity in their slopes reveals the extent to which the dependence of these parameters on the nuclear mass number (A) is comparable, highlighting their universality.

These observations are consistent with the hypothesis that the SRC pairs are dominantly protonneutron combinations.

**Figure 1-b):** Focusing on the lower panel, Figure 1-b) we display the  $C_p^A$  coefficients for the baseSRC. We also show the logarithmic fits for both baseSRC and pnSRC and they closely coincide. Additionally, we overlay predictions from independent, extractions from both nuclear structure calculations [7] and quasi-elastic electron scattering measurements [4–6].

This behavior is consistent with the observed *pn*-dominance previously established in nuclear structure studies [10, 11]. Consequently, the agreement between the baseSRC and pnSRC fits provides an initial indication of consistency between quark–gluon–level analyses and traditional nuclear structure observations.

#### **Conclusion:**

We have presented a novel paradigm that directly links nuclear structure information to parton (quark and gluon) dynamics. This framework enables the first direct extraction of nPDFs that is fully consistent with independent nuclear structure determinations.

This analysis yields a data description that is similar to or better than that of the traditional parameterization and enables a meaningful physical interpretation of the fit in terms of the nuclear

dynamics. The study successfully determines both the standard "average" nPDFs (which can be directly compared with traditional nPDF fits), and the universal distribution of partons in SRC nucleon pairs, along with the fractions of such SRC pairs.

The agreement between the SRC fractions derived here and those obtained from low-energy quasielastic measurements establishes a clear connection between high-energy partonic behavior and low-energy nuclear structure, marking a significant step toward understanding nuclei in terms of partonic QCD processes.

The SRC framework provides additional flexibility by allowing one to (i) follow the traditional approach using averaged nucleon distributions, or (ii) construct a more detailed initial-state description in which each nucleon is represented by either a free-nucleon PDF or an SRC-modified PDF, depending on its correlation state.

Furthermore, it is noteworthy that the SRC parameterization (in which the dependence of A and x is factorized) produces an excellent description of the data. The conceptual simplicity of this successful parameterization is striking.

#### Acknowledgment:

This study was performed in collaboration with members of the nCTEQ Collaboration and Or Hen's MIT research group. We are grateful to Tim Hobbs, Jeff Owens and Efrain Segarra for valuable discussion. This work was supported by the U.S. DoE Grant No. DE-SC0010129, and by the U.S. DoE, Office of Science, Office of Nuclear Physics, within the framework of the Saturated Glue (SURGE) Topical Theory Collaboration. This work was performed in part at the Aspen Center for Physics, which is supported by National Science Foundation grant PHY-2210452.

#### References

- [1] A. W. Denniston *et al.* (nCTEQ), Phys. Rev. Lett. **133**, 152502 (2024), arXiv:2312.16293 [hep-ph].
- [2] K. Kovarik et al. (nCTEQ), Phys. Rev. D 93, 085037 (2016), arXiv:1509.00792 [hep-ph].
- [3] M. Klasen, in 32nd International Workshop on Deep-Inelastic Scattering and Related Subjects (2025) arXiv:2510.05880 [hep-ph].
- [4] K. S. Egiyan et al. (CLAS), Phys. Rev. Lett. 96, 082501 (2006), arXiv:nucl-ex/0508026.
- [5] N. Fomin et al., Phys. Rev. Lett. 108, 092502 (2012), arXiv:1107.3583 [nucl-ex].
- [6] B. Schmookler et al. (CLAS), Nature 566, 354 (2019), arXiv:2004.12065 [nucl-ex].
- [7] R. Cruz-Torres et al., Nature Phys. 17, 306 (2021), arXiv:1907.03658 [nucl-th].
- [8] P. Paakkinen, (2025), arXiv:2510.00252 [hep-ph].
- [9] E. P. Segarra et al., Phys. Rev. D 103, 114015 (2021), arXiv:2012.11566 [hep-ph].
- [10] R. Subedi et al., Science 320, 1476 (2008), arXiv:0908.1514 [nucl-ex].
- [11] E. Piasetzky et al., Phys. Rev. Lett. 97, 162504 (2006), arXiv:nucl-th/0604012.